Published in final edited form as:
Magn Reson Med. 2003 February ; 49(2): 216–222.

Undersampled Projection Reconstruction for Active Catheter Imaging With Adaptable Temporal Resolution and Catheter-Only Views

Dana C. Peters[1,*], **Robert J. Lederman**[2], **Alexander J. Dick**[2], **Venkatesh K. Raman**[2], **Michael A. Guttman**[1], **J. Andrew Derbyshire**[1], and **Elliot R. McVeigh**[1]

[1]*Laboratory of Cardiac Energetics, National Institutes of Health, Bethesda, Maryland.* [2]*Cardiovascular Branch, National Institutes of Health, Bethesda, Maryland.*

Abstract

In this study undersampled projection reconstruction (PR) was used for rapid catheter imaging in the heart, employing steady-state free precession (SSFP) contrast. Active catheters and phased-array coils were used for combined imaging of anatomy and catheter position in swine. Real-time imaging of catheter position was performed with relatively high spatial and temporal resolution, providing 2 × 2 × 8 mm spatial resolution and four to eight frames per second. Two interactive features were introduced. The number of projections (Np) was adjusted interactively to trade off imaging speed and artifact reduction, allowing acquisition of high-quality or high-frame-rate images. Thin-slice imaging was performed, with interactive requests for thick-slab projection images of the signal received solely from the active catheter. Briefly toggling on catheter-only projection images was valuable for verifying that the catheter tip was contained within the selected slice, or for locating the catheter when part of it was outside the selected slice.

Keywords

catheter tracking; interventional MRI; projection reconstruction; radial imaging; real-time MRI; intravascular MRI; MR fluoroscopy; cardiac MRI

A crucial feature of vascular interventional procedures is catheter or guidewire imaging or tracking. This requires good contrast, and high temporal and spatial resolution for the device and surrounding anatomy. One important obstacle in MRI is that increased spatial resolution is often obtained at the cost of increased scan time (i.e., decreased temporal resolution). It is also sometimes difficult to observe the distal portion and catheter tip during catheter manipulations in the acquired slice, because the catheter tip often lies outside of the slice. These challenges regarding high temporal and spatial resolution, and device localization in a thin slice were addressed using undersampled projection reconstruction (PR), or radial imaging, for active catheter imaging in the aorta and cardiac chambers.

Different interventional tasks have different imaging requirements. For example, gross catheter movements in the aorta require high temporal resolution. Fine device placement (such as selective artery engagement or stent placement) requires high image quality, which may come at the expense of temporal resolution. Undersampled PR acquires radial lines of *k*-space

[*]Correspondence to: Dana C. Peters, National Institutes of Health, 10 Center Drive, Bldg. 10 B1D416, Bethesda, MD 20892-1061. E-mail: petersd@nih.gov

(projections). PR permits the independent adjustment of temporal resolution at constant spatial resolution, by reducing the number of projections (Np); however, aliasing artifacts may appear. For PR, the spatial resolution is determined primarily by the readout resolution (Nr), while the Np determines the level of artifact (1). Reduction of Np provides improved temporal resolution, decreases SNR by the square root of scan time, increases artifacts due to undersampling, and results in little change in the nominal spatial resolution.

The present investigation employed combined imaging of an active catheter and anatomy using a phased-array coil, in a *thin* slice. The catheter acted as a coil tuned to receive MR signal throughout its length. Neither thin-slice nor thick-slab projection imaging is optimal for visualizing invasive devices. In thin-slice imaging, only a section of the active catheter is imaged, since only a portion of the catheter is located within the slice. Thick-slab projection images contain the entire catheter, but the anatomical context is blurred due to partial voluming of features. Thick-slab projection images of the catheter overlaid on an anatomical roadmap provide unreliable (semi-static) or no anatomical context, especially when monitoring therapy delivery, such as by injection. This work presents a new interactive feature for visualizing the entire device during thin-slice imaging, whereby one briefly toggles on a thick-slab image, and reconstructs only the catheter coil channel.

In this study we employed MR catheter imaging in the cardiac chambers. Potential MR-guided interventional applications for catheter-based interventions in this region include endocardial injection of therapeutic agents, e.g., angiogenic therapies (2), catheter ablations in rhythmn disorders, and transcatheter valve replacement (3).

METHODS

Imaging was performed on a General Electric (Waukesha, WI) CV/i 1.5 T system. A commercial fast gradient-echo sequence was modified to collect projections and provide gradient-echo or steady-state free precession (SSFP) contrast with short TRs. Full echoes were collected at evenly spaced angles over 180°. SSFP contrast provides bright blood and high SNR, and is useful for interventional MRI (4). The scan parameters used for all PR images were: Nr = 160, field of view (FOV) = 32 cm, slice thickness = 8 mm, flip angle = 50°, receiver bandwidth = ±62.5 kHz, TR = 4.1 ms. The slice thickness was increased by a factor of 4 for catheter-only projection images, and the number of projections (Np) was interactively varied, but ranged between 32 and 128. This imaging sequence was employed in conjunction with the scanner's real-time imaging and interactive scan plane adjustment package (iDrive). When gradient waveform updates (concerning, for example, slice thickness changes, scan plane changes, or change in Np) were requested, interscan delays of 40 ms were placed between images to provide time for calculation of gradient waveforms, and receiver phases and frequencies. After interscan delays, $\alpha/2$ preparatory pulses were used (5), followed by eight dummy TRs, in order to better approach a steady state for SSFP. When updates were not necessary, no interscan delays or preparatory pulses were placed between frames, providing a true steady state. This was valuable when imaging was performed with very few projections (<48 Np).

The “active” catheter used in these experiments was a guiding catheter coil with inner (7 F) and outer (9 F) braided conductors (Boston Scientific, Watertown, MN) (2,6). This was connected to a four-input phased-array coil (Nova Medical, Inc., Wakefield, MA), with four pre-amps that were designed for high impedance to minimize inductive coupling among coils. One of the four surface coils was removed and replaced with the catheter coil. The remaining surface coils were used for anatomical imaging. The catheter channel was isolated so as to allow independent amplification and color-coding of the catheter channel (7,8).

Real-Time PR Image Reconstruction

To permit the use of the interactive scan plane prescription utilities (iDrive; GE), an online regridding reconstruction, intended for spiral imaging, was enabled for PR. The PR *k*-space trajectory was provided as a file to the regrid-ding reconstruction. The regridding was performed with a convolution function (width = 2 pixels), without subsampling of the *k*-space data onto a finer array. This provided image updates at a rate sufficient to allow interactive prescription of slices.

In addition to the online scanner reconstruction, a remote workstation-based real-time reconstruction (9,10) allowed more rapid, customized image reconstruction and display, and provided an interactive environment for pulse sequence control. A Bit3 bus adapter (SBS Technologies) was used to obtain raw image data from scanner memory, and to send commands. Reconstruction and display were performed using a multithreaded open GL application on an Onyx2 Reality Engine (Silicon Graphics, Inc.). The maximum reconstruction frame rate (independent of acquisition frame rate) was 8–10 frames per second (fps), with a latency of <300 ms (160 Nr × 32 Np, four coils). Regridding was performed using a triangular convolution function (width = 2 pixels) (11). Fourier transforms were performed using FFTW software (www.fftw.org). The images from both reconstructions were displayed and the scanner was interactively controlled using two MR-compatible in-room consoles (Aydin Displays, Horsham, PA) situated approximately 1 m outside of the scanner bore.

Interactive Features: Adjustable Temporal Resolution

Interactive features were added for catheter tracking, using simple in-room keyboard commands. One feature allowed interactive change in the Np acquired (see Fig. 1), ranging between Np_{max} (the prescribed Np) and one-quarter of Np_{max}, in eight projection increments. This increment was chosen as a reasonable step size, but in practice any step size can be used. Imaging with a modified Np was achieved by communicating with the pulse sequence in real time to recompute gradient waveforms, and receiver phase and frequency values, for acquisition of a different Np. If high numbers of projections were desired, the adjustable temporal resolution was used in conjunction with interactively requested ECG-gating, whereby a fraction of the projections were acquired in consecutive heartbeats.

Catheter-Only Views Using Increased Slice Thickness and Coil Isolation

Another interactive feature allowed changes in slice thickness, using modifications of slice-select gradients in real time. This was practically limited so that the initially prescribed slice thickness was the minimum slice thickness. The device channel could be isolated by increasing slice thickness by a factor of 4 and requesting reconstruction of only the device channel. This provided catheter-only views, in which the entire length of the catheter was shown.

Interventional Experiments

All protocols were approved by our institutional Animal Care and Use Committee. Catheterization was performed in swine, as described elsewhere (2). An active catheter was guided into the aorta, using MR image guidance. Real-time PR catheter tracking was performed in the aorta, aortic arch, and left ventricular cavity. Real-time Cartesian catheter tracking, as recently presented by our group (2,12), was also performed and compared with PR.

Endomyocardial injections were performed by inserting an injection needle (Stiletto; Boston Scientific) (6) into the active guiding catheter, and injecting into the myocardium 0.5 ml of 30 mM gadolinium contrast agent under MR guidance (2). Immediately before injection, by interactive request, a nonselective 90° RF pulse was used for magnetization preparation, and

after a delay of roughly 20 ms, spoiled gradient-echo imaging was employed. This provided T_1 weighting for detecting the gadolinium contrast agent.

RESULTS

The catheter appeared in the images as a bright halo surrounding a dark core. The coil sensitivity pattern varied along the catheter length and according to catheter coil orientation with respect to the main magnetic field. Whenever the catheter was in proximity of the image plane, the signal received was sufficient for localizing the catheter.

Figure 2 shows three consecutive frames of device tracking in the left ventricular cavity, spanning 590 ms. The active device is indicated by the arrow. The device was observed to move rapidly through the aortic valve. The spatial resolution of the images was 2 × 2 × 8 mm, and the temporal resolution was 197 ms per frame (5.1 fps). Some motion artifact is evident (see Discussion).

Figure 3 shows the utility of catheter-only views. The image in Fig. 3a shows a portion of the catheter (the thick arrow indicates the *apparent* tip of the catheter), but the position of the tip and the path of the catheter are not clear. The catheter-only mode of imaging was invoked interactively using an in-room keyboard command (Fig. 3b), causing a fourfold increase in slice thickness (from 8 to 32 mm), and reconstruction of only the catheter channel. The catheter-only image, obtained about one-half second after the thin-slice image, shows the entire catheter. Only a portion of the catheter had been observed in the thin slice. The thick arrows indicate identical positions in the FOV. The thin arrow points roughly to the true catheter tip.

Figure 4 compares Cartesian and PR acquisitions with approximately equal scan times (3.8 fps for Cartesian, 5.1 fps for PR). The PR image has higher acquired spatial resolution (2 × 2 × 8 mm) compared to the Cartesian image (1.9 × 3.7 × 8 mm), but has some artifacts. The images were obtained in the same animal at identical slice orientations. The catheter is observed in both images.

The appearance of the catheter positioned in the left ventricle at different levels of undersampling can be observed in Fig. 5. This shows a long-axis view of the left ventricle and ascending aorta with (a) 32 Np (8 fps), (b) 48 Np (5 fps), and (c) 64 Np (4 fps). Figure 5 shows the moderate improvement in image quality, due to higher SNR and fewer artifacts, with the inclusion of progressively more projections. Inspection of Fig. 5 shows that the catheter itself was a source of undersampling artifacts. This was as expected, because linear objects produce prominent streaking artifacts when subject to undersampling. The sharpness of the catheter was improved by the reduction of motion blur when Np was reduced. These images were acquired during continuous scanning. A movie loop of these images can be viewed on the Internet at http://rover.nhlbi.nih.gov/labs/papers/lce/petersd1.html. The movie loop demonstrates the trade-offs permitted by adjustable temporal resolution, which result in smoother depiction of motion using fewer projections, and fewer aliasing artifacts with more projections.

Figure 6 shows the value of adjustable temporal resolution. The catheter was positioned toward the apex of the heart, and an injection needle was guided through it and deployed at the myocardial border (arrow in Fig. 6a), using real-time imaging with 40 Np. Prior to injection of gadolinium contrast agent into the endocardium, image contrast was interactively modified for T_1 weighting, as described in Methods. The image acquired with 40 Np (Fig. 6b) shows a bright region marking the injection site. With the use of more Nps (64 Np in Fig. 6c), the injection could be seen more clearly, because SNR was increased and artifacts were reduced.

DISCUSSION

Several properties of the PR trajectory contribute to its usefulness in rapid device imaging. In the PR acquisition, low spatial frequency information is obtained in each acquisition, significantly updating the image with the inclusion of each new projection. This results in more temporal averaging of the catheter image. It also provides the opportunity for a sliding window reconstruction (13,14) centered around any time point. Motion artifacts are different for the PR trajectory, compared with Cartesian trajectories. Objects in motion during the acquisition of an image are blurred (for example, the catheter in Fig. 2b) due to inter-projection inconsistencies that depend on the details of the motion. However, the moving objects only cause low-intensity streaks on the rest of the FOV (Fig. 2b), unlike Cartesian acquisitions wherein ghosting artifacts are more visible (15).

In previous studies (16-19), as in the present work, imaging of the cardiac chambers was performed with PR using 128–256 readout resolution (Nr) and about 50 projections (Np). That is an undersampling factor ($U = (\pi Nr)/(2Np)$) of about 3–6. In the present study, undersampling factors of 3–7 were used for combined device and anatomy imaging. Compared to Cartesian imaging of equal spatial resolution, this provides an increase in speed (Nr/Np) by a factor of 2–5. However, Cartesian imaging can employ fractional FOVs and half-Fourier techniques to reduce imaging time, as in the comparison shown in Fig. 4. Figure 4 indicates that, compared to Cartesian imaging, undersampled PR can provide higher resolution for catheter tracking, as demonstrated by the sharper catheter appearance. However, further work is required to quantitatively compare the differences in temporal and spatial resolution between PR and Cartesian acquisitions for active catheter tracking. Phantom experiments could demonstrate how the temporal differences between the two *k*-space collection methods affect catheter temporal blurring, and whether the improved spatial resolution of PR provides quantitatively improved catheter delineation.

Device imaging and tracking with PR was previously investigated using passive devices: catheters filled with gadolinium contrast agent (20), susceptibility-guided stent placements (21), and needle tracking with susceptibility contrast (13,22,23). Tracking of microcoils (13, 24,25), involving imaging of bright spots, has also been achieved using PR with just a few projections (26,27). The present investigation differs from previous studies in that PR was employed with greater undersampling factors, active catheters combined with anatomy were imaged, and adjustable temporal resolution was employed.

In this investigation we observed interactive changes of temporal resolution during continuous scanning, using adjustments of Np. In contrast to techniques that interleave projections and then reconstruct each set singly or in combination (18,28), the present method collects any Np, on request. The PR trajectory has the characteristic that the temporal resolution can be modified without reduction in nominal spatial resolution (see Figs. 5 and 6), although in some situations, artifacts and reduced SNR reduce the image quality. This feature is useful for imaging-device manipulation at high frame rates followed by slower high-quality imaging (Fig. 6). When switching scan plane orientation, Np can be adjusted to provide the preferred trade-off between artifacts and temporal resolution, as required by that scan plane. For example, 32 projections provide relatively artifact-free images for the short-axis view in Fig. 1, but less tolerable artifacts for the long-axis image in Fig. 5, because more projections are required to suppress aliasing artifacts from the catheter. Cartesian acquisitions could also benefit from this adaptibility because the numbers of phase-encodings could be changed interactively, and thus resolution could be adjusted in the phase-encoding direction. However, reduced phase-encoding methods cannot employ reduced FOVs unless unaliasing techniques are used (29).

In thin-slice combined imaging of catheters and anatomical context, there is uncertainty about the position of the tip of the catheter. For this reason, previous investigations of active device tracking with MRI have focused on thick-slab projection methods whereby the entire device or the microcoil position is observed in a thick slab, and the intravascular device is used as an MRI receiver (8,26). The resulting images are similar to X-ray because they display the length of the intravascular device or position of the fiducial. However, the anatomical structures are either blurred due to a thick acquired slab or only represented by a static or semi-static roadmap of anatomy. The present investigation provides a new, interactive solution to this problem by using thin slices, but permitting instantaneous thick slab catheter only images by request (Fig. 3). These images instantly display the entire length of the catheter and guarantee visualization of the tip, if signal is received there.

Active-device tracking is challenging. This investigation employed high temporal and spatial resolution to image the device and anatomy simultaneously, with some under-sampling artifacts. Thick-slab, catheter-only images were valuable for locating the catheter when part of it was outside the slice. When a single, higher-quality image of the anatomy or device was required, an interactively requested image was obtained using more projections to obtain better SNR and image quality. This is a simple and effective approach to catheter tracking and imaging. In our experience, PR has unique features that are well suited for visualization of distal portions of the catheter, which is crucial for vascular interventional procedures.

ACKNOWLEDGMENTS

The authors thank Joni Taylor, Diana Lancaster, and Gina Orcino (NIH) for animal care, Daniel Herzka (NIH) for helpful suggestions, and Patrick Ledden (Nova Medical, Inc.) and Peter Kellman (NIH) for providing the custom phased-array coil. The authors also thank Scott Smith and Ken Larson (Boston Scientific Scimed) for providing the active catheters.

REFERENCES

1. Peters DC, Korosec FR, Grist TM, Block WF, Holden JE, Vigen KK, Mistretta CA. Undersampled projection reconstruction applied to MR angiography. Magn Reson Med 2000;43:91–101. [PubMed: 10642735]
2. Lederman RJ, Guttman MA, Peters DC, Thompson RB, Sorger JM, Dick AJ, Raman VK, McVeigh ER. Catheter-based endomyocardial injection with real-time magnetic resonance imaging. Circulation 2002;105:1282–1284. [PubMed: 11901036]
3. Boudjemline Y, Bonhoeffer P. Steps toward percutaneous aortic valve replacement. Circulation 2002;105:775–778. [PubMed: 11839637]
4. Duerk JL, Lewin JS, Wendt M, Petersilge C. Remember true FISP? A high SNR, near 1-second imaging method for T2-like contrast in interventional MRI at .2 T. J Magn Reson Imaging 1998;8:203–208. [PubMed: 9500281]
5. Deimling, M.; Heid, O. Magnetization prepared true FISP imaging; Proceedings of the 2nd Annual Meeting of SMRM; San Francisco. 1994. p. 495
6. Grossman PM, Han Z, Palasis M, Barry JJ, Lederman RJ. Incomplete retention after direct myocardial injection. Cath Cardiovasc Interv 2002;55:392–397.
7. Guttman, MA.; Sorger, JM.; McVeigh, ER. Real-time volumetric MR imaging; Proceedings of the 9th Annual Meeting of ISMRM; Glasgow, Scotland. 2001. p. 598
8. Serfaty JM, Yang X, Aksit P, Quick HH, Solaiyappan M, Atalar E. Toward MRI-guided coronary catheterization: visualization of guiding catheters, guidewires, and anatomy in real time. J Magn Reson Imaging 2000;12:590–594. [PubMed: 11042641]
9. Guttman MA, McVeigh ER. Techniques for fast stereoscopic MRI. Magn Reson Med 2001;46:317–323. [PubMed: 11477636]
10. Kerr AB, Pauly JM, Hu BS, Li KC, Hardy CJ, Meyer CH, Macovski A, Nishimura DG. Real-time interactive MRI on a conventional scanner. Magn Reson Med 1997;38:355–367. [PubMed: 9339436]

11. Jackson JI, Meyer CH, Nishimura DG. Selection of a convolution function for Fourier inversion using gridding. IEEE Trans Med Imaging 1991;10:473–478. [PubMed: 18222850]
12. Guttman, MA.; Kellman, P.; McVeigh, ER. Real-time interactive accelerated imaging with on-line adaptive TSENSE; Proceedings of the 10th Annual Meeting of ISMRM; Honolulu. 2002. p. 195
13. Rasche V, de Boer RW, Holz D, Proksa R. Continuous radial data acquisition for dynamic MRI. Magn Reson Med 1995;34:754–761. [PubMed: 8544697]
14. Riederer SJ, Tasciyan T, Farzaneh F, Lee JN, Wright RC, Herfkens RJ. MR fluoroscopy: technical feasibility. Magn Reson Med 1988;8:1–15. [PubMed: 3173063]
15. Glover GH, Pauly JM. Projection reconstruction techniques for reduction of motion effects in MRI. Magn Reson Med 1992;28:275–289. [PubMed: 1461126]
16. Peters DC, Epstein FH, McVeigh ER. Myocardial wall tagging with undersampled projection reconstruction. Magn Reson Med 2001;45:562–567. [PubMed: 11283982]
17. Barger AV, Grist TM, Block WF, Mistretta CA. Single breath-hold 3D contrast-enhanced method for assessment of cardiac function. Magn Reson Med 2000;44:821–824. [PubMed: 11108617]
18. Schaeffter T, Weiss S, Eggers H, Rasche V. Projection reconstruction balanced fast field echo for interactive real-time cardiac imaging. Magn Reson Med 2001;46:1238–1241. [PubMed: 11746592]
19. Shankaranarayanan A, Simonetti OP, Laub G, Lewin JS, Duerk JL. Segmented k-space and real-time cardiac cine MR imaging with radial trajectories. Radiology 2001;221:827–836. [PubMed: 11719686]
20. Unal, O.; Peters, DC.; Korosec, FR.; Frayne, R.; Block, WF.; Mistretta, CA.; Grist, TM.; Strother, CM. Angular projection MR techniques for passive catheter tracking; Proceedings of the 7th Annual Meeting of ISMRM; Philadelphia. 1999. p. 946
21. Spuentrup E, Ruebeen A, Schaeffter T, Manning WJ, Gunther RW, Buecker A. Magnetic resonance-guided coronary artery stent placement in a swine model. Circulation 2002;105:874–879. [PubMed: 11854130]
22. Shankaranarayanan A, Wendt M, Aschoff AJ, Lewin JS, Duerk JL. Radial keyhole sequences for low field projection reconstruction interventional MRI. J Magn Reson Imag 2001;13:142–151.
23. Shimizu K, Mulkern RV, Oshio K, Panych LP, Yoo SS, Kikinis R, Jolesz FA. Rapid tip tracking with MRI by a limited projection reconstruction technique. J Magn Reson Imag 1998;8:262–264.
24. Rasche V, Holz D, Kohler J, Proksa R, Roschmann P. Catheter tracking using continuous radial MRI. Magn Reson Med 1997;37:963–968. [PubMed: 9178250]
25. Buecker A, Neuerburg JM, Adam GB, Glowinski A, Schaeffter T, Rasche V, van Vaals JJ, Molgaard-Nielsen A, Guenther RW. Real-time MR fluoroscopy for MR-guided iliac artery stent placement. J Magn Reson Imaging 2000;12:616–622. [PubMed: 11042645]
26. Dumoulin CL, Souza SP, Darrow RD. Real-time position monitoring of invasive devices using magnetic resonance. Magn Reson Med 1993;29:411–415. [PubMed: 8450752]
27. Flask C, Elgort D, Wong E, Shankaranarayanan A, Lewin J, Wendt M, Duerk JL. A method for fast 3D tracking using tuned fiducial markers and a limited projection reconstruction FISP (LPR-FISP) sequence. J Magn Reson Imaging 2001;14:617–627. [PubMed: 11747015]
28. Song HK, Dougherty L, Schnall MD. Simultaneous acquisition of multiple resolution images for dynamic contrast enhanced imaging of the breast. Magn Reson Med 2001;46:503–509. [PubMed: 11550242]
29. Atalar E, Kraitchman DL, Carkhuff B, Lesho J, Ocali O, Solaiyappan M, Guttman MA, Charles HK Jr. Catheter-tracking FOV MR fluoroscopy. Magn Reson Med 1998;40:865–872. [PubMed: 9840831]

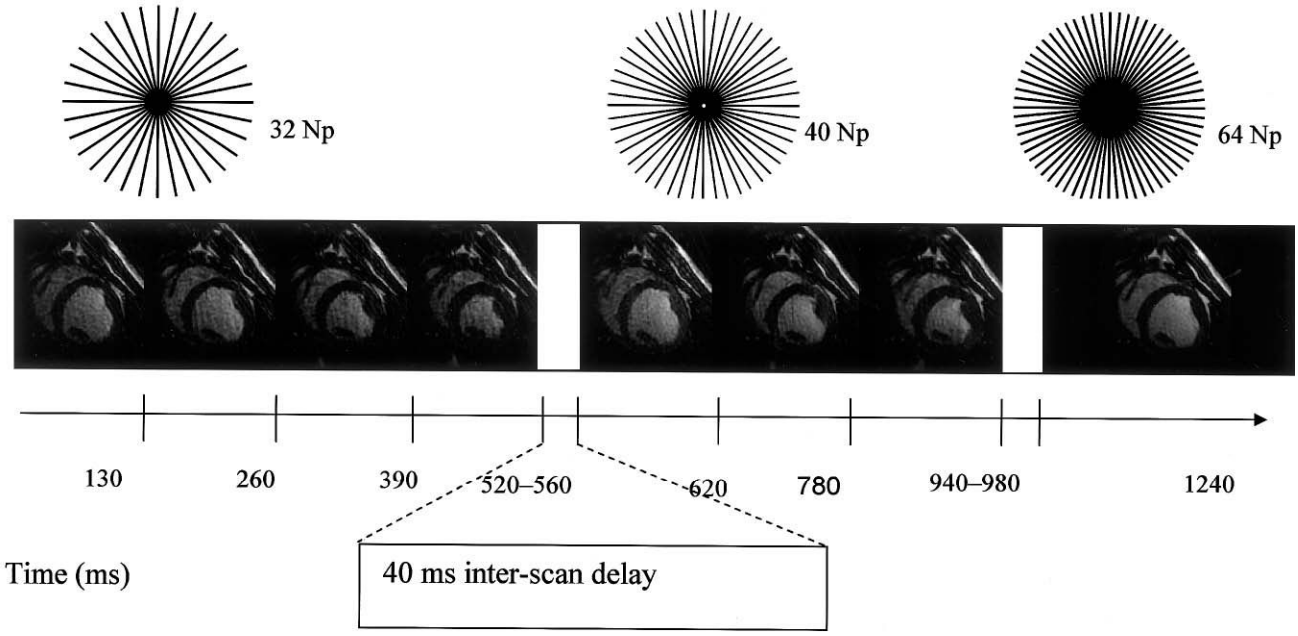

FIG. 1.

Real-time interactive adjustment of temporal resolution is shown schematically. Imaging can be performed using any Np, during uninterrupted scanning. The Np is increased or decreased using a simple keyboard command. Here 32 projections and a 4-ms TR were used to acquire a number of short-axis cardiac images rapidly; Np was then increased to 40, and a 64-Np frame was obtained. During the 40-ms interscan delays, all of the necessary updates to gradient waveforms, and receiver phase and frequency tables were performed for acquisition with an adjusted Np.

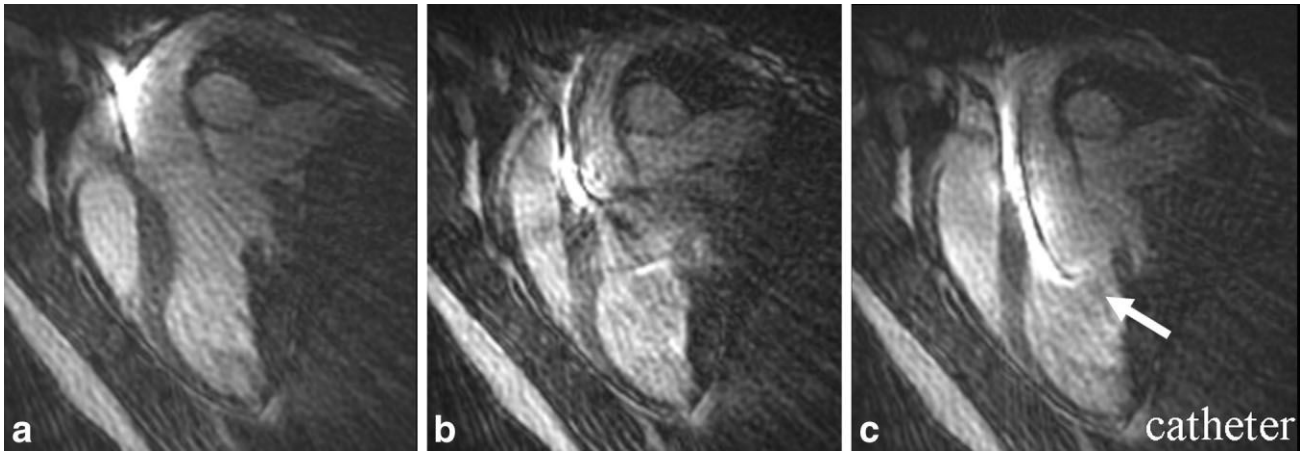

FIG. 2.

A zoomed view of the left ventricular cavity and ascending aorta. The catheter (arrow) was visualized in three consecutive frames, as the catheter device was navigated through the aortic arch into the left ventricular cavity using 196-ms temporal resolution, 48 projections, and 2 × 2 × 8 mm spatial resolution. Note the sharp visualization of the entire length of the active device, and the endocardial wall. Motion artifact is observed in the central image, due to the rapidly moving catheter (see Discussion).

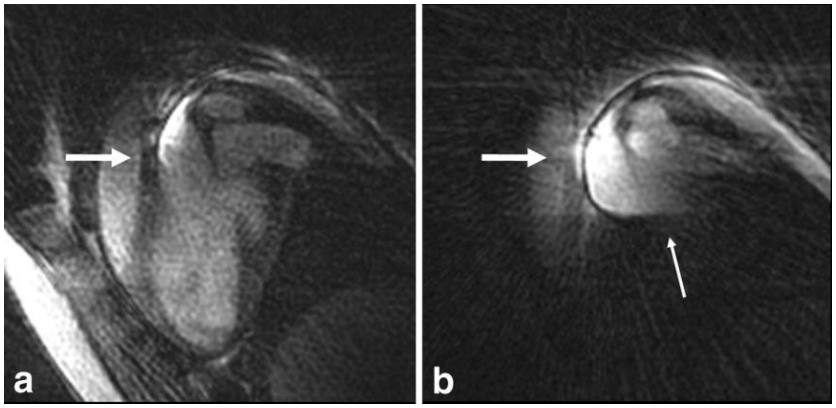

FIG. 3.

Catheter-only mode. **a:** A thin slice reveals part of the catheter (bright signal marked by the arrow indicates the apparent tip of the catheter) with respect to the anatomy; however, it was unclear whether the distal tip shown in this slice is the actual tip of the catheter, or the catheter tip was outside of the selected slice. **b:** Less than a half second later, the slice thickness was increased by a factor of 4, and the catheter channel was reconstructed alone, so that the entire active device was visualized by interactive request. The thick arrows point to identical positions in the FOV. The thin lower arrow in **b** points roughly toward the true catheter tip. A total of 64 projections were used.

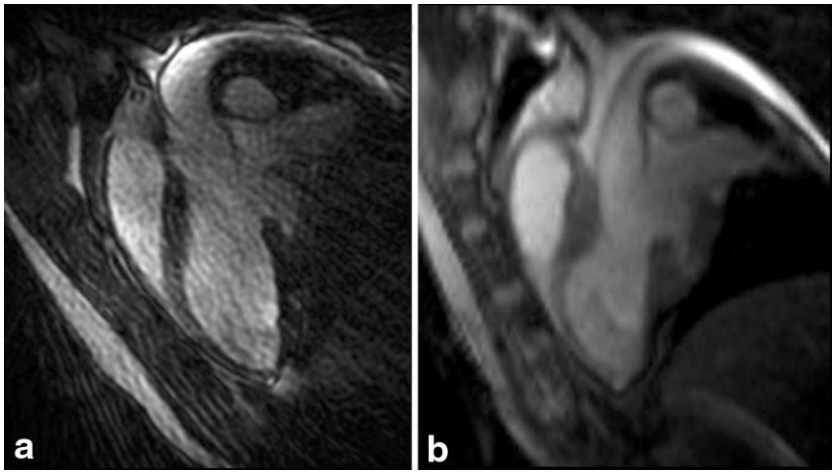

FIG. 4.

Comparison of catheter tracking with (**a**) PR and (**b**) Cartesian acquisitions, showing a single frame from real-time imaging in the same pig with each trajectory, at the same slice orientation. Imaging parameters for PR were: FOV = 32 cm, slice thickness = 8 mm, 160 Nr × 48 Np, receiver bandwidth = ±62.5 kHz, TR/θ = 4.1 ms/50°, resulting in 2 × 2 × 8 mm spatial resolution and 5.1 fps. For Cartesian: FOV = 36 cm, slice thickness = 8 mm, 192 Nx × 96 Ny, FOV = ¾ (72 views), receiver bandwidth = ±125 kHz, TR/θ = 3.7 ms/60°, resulting in 1.8 × 3.7 × 8 mm spatial resolution and 3.8 fps. SSFP was employed for both acquisitions.

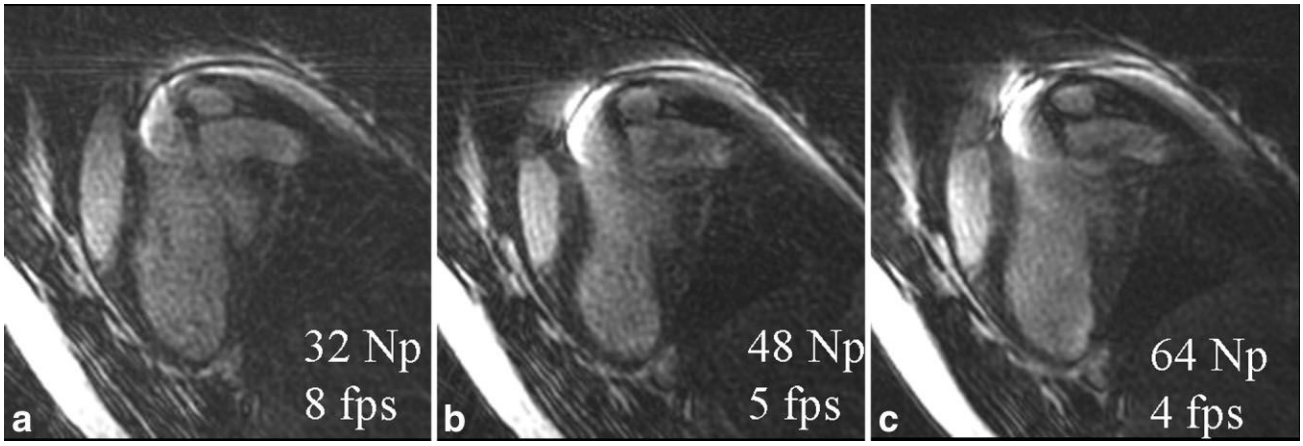

FIG. 5.

A series of long-axis images acquired about 5–10 s apart during continuous scanning, with 160 Nr and (**a**) 32 Np (7.6 fps), (**b**) 48 Np (5.1 fps), and (**c**) 64 Np (3.8 fps). Note the minor changes in artifact (especially radiating from the catheter) and SNR.

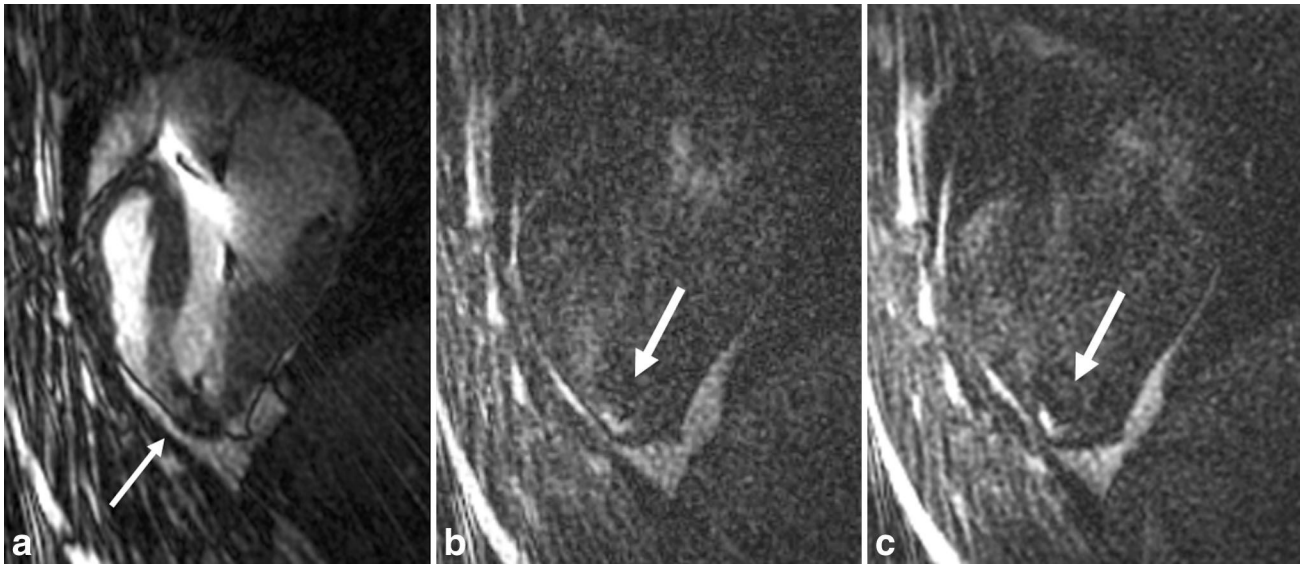

FIG. 6.

a: A catheter (arrow indicates tip) was positioned toward the apex of the heart, imaged with 40 Np (164 ms temporal resolution). **b:** An injection of gadolinium (arrow) was made into the endocardium and observed with T_1-weighted imaging, imaged with 40 Np (164 ms). **c:** The injection was imaged interactively with 64 Np (262 ms), providing higher SNR and fewer artifacts.